

See discussions, stats, and author profiles for this publication at: <https://www.researchgate.net/publication/231706328>

# Critical Strain for Shish-Kebab Formation

ARTICLE *in* MACROMOLECULES · DECEMBER 2009

Impact Factor: 5.8 · DOI: 10.1021/ma9020642

---

CITATIONS

45

---

READS

55

10 AUTHORS, INCLUDING:



**Liangbin Li**

University of Science and Technology of China

137 PUBLICATIONS 2,045 CITATIONS

SEE PROFILE



**Xiuhong Li**

Shanghai Institute of Applied Physics

38 PUBLICATIONS 316 CITATIONS

SEE PROFILE



**Fenggang Bian**

Shanghai Institute of Applied Physics

21 PUBLICATIONS 85 CITATIONS

SEE PROFILE

## Critical Strain for Shish-Kebab Formation

Tingzi Yan,<sup>†</sup> Baijin Zhao,<sup>†</sup> Yuanhua Cong,<sup>†</sup> Yuye Fang,<sup>‡</sup>  
Shiwang Cheng,<sup>‡</sup> Liangbin Li,<sup>\*,†,‡</sup> Guoqiang Pan,<sup>†</sup>  
Zijian Wang,<sup>‡</sup> Xiuhong Li,<sup>§</sup> and Fenggang Bian<sup>§</sup>

<sup>†</sup>National Synchrotron Radiation Lab and College of Nuclear Science and Technology, University of Science and Technology of China, Hefei, China, <sup>‡</sup>CAS Key Lab for Softmatter Chemistry, University of Science and Technology of China, Hefei, China, and <sup>§</sup>Shanghai Synchrotron Radiation Facility, Shanghai, China

Received September 16, 2009

Revised Manuscript Received December 22, 2009

**ABSTRACT:** A combination of extensional rheological and in situ synchrotron radiation small-angle X-ray scattering (SR-SAXS) measurements was introduced to investigate critical strain  $\epsilon^*$  for shish formation and validate whether coil–stretch transition or stretched-network is responsible for shish-kebab formation in high density polyethylene melt. With strain rates  $\dot{\epsilon}$  larger than a specific value, the critical strain  $\epsilon^*$  required to induce shish formation turns out to be a constant of about 1.57, which ensure full extension of chain segments with critical entanglement molecular weight locked between two adjacent entanglement points. The results clearly demonstrate that the formation of shish-kebab in polymer melt stems from stretched network instead of coil–stretch transition.

**Introduction.** Flow-induced polymer crystallization is of vital importance in polymer processing, because nearly all polymers are under complex flow fields before they become products.<sup>1</sup> It has been confirmed for decades that flow can enhance polymer crystallization<sup>2,3</sup> and sometimes make the crystal morphology change from spherulites to shish-kebab structures.<sup>2,4</sup> The shish-kebab structure was first observed in the 1960s individually by Mitsuhashi, Pennings and Binsbergen et al.<sup>5–7</sup> Since then, great interest has been paid to the shish-kebab structure, not only for the property enhancement of commercial products but also for the underlying nonthermodynamic physical mechanism.<sup>8–10</sup> However, the mechanism of shish-kebab formation is still unclear and under open debate.

On the basis of the duality of the shish-kebab superstructure observed in polymer solution and melt, Keller introduced de Gennes's coil–stretch transition<sup>11</sup> concept in the polymer solution to interpret flow-induced shish-kebab morphology in the polymer melt,<sup>12</sup> which has been widely accepted in the community.<sup>13–16</sup> In Keller's view, under a specific flow polymer chains with molecular weight higher than a critical molecular weight  $M^*$  can be stretched and the rest shorter chains remain in the coiled state. The former forms the extended shish crystal and the later forms the folded chain lamellae, i.e., the kebab.

In fact, the long-standing concept for shish-kebab formation that the chain should be stretched out to undergo the coil–stretch transition has always been questioned. Pennings believed that stretched network is responsible for shish formation,<sup>17</sup> which was also suggested recently by Zhang et al.<sup>18</sup> Recent small angle neutron scattering experiments revealed that shish composes of not only long chains but also short ones,

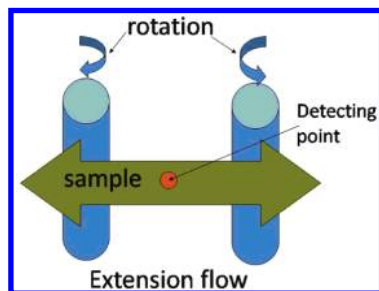
which is difficult to reconcile with the coil–stretch transition model.<sup>19</sup> Alternatively, the coil–stretch transition of sections of chains instead of the whole chain was proposed by some groups.<sup>20–22</sup> Nevertheless, due to experimental difficulties, direct experimental evidence to justify whether the coil–stretch transition or stretched network is responsible to shish-kebab formation in polymer melt is still absent.<sup>12</sup>

In this communication, we focus on two questions related to the mechanism of shish-kebab formation. (i) Is a critical strain required for shish-kebab formation? (ii) Is coil–stretch transition a necessary condition for shish-kebab formation? A combination of in situ extensional rheological measurement and synchrotron radiation small-angle X-ray scattering (SR-SAXS) is introduced to answer these two questions. As polymer melt is a transient network constructed with entangled polymer chains, the occurrence of coil–stretch transition in polymer melt means that polymer chains have to be stretched out from the original tube formed by their neighbor chains with topological entanglement, which undergoes a disentanglement process. This process is manifested through microscopically cohesive failure and macroscopically necking or yield during extensional rheological measurements.<sup>23</sup> Thus, the occurrence of the coil–stretch transition can be justified by extensional rheological measurements. On the other hand, the formation of shish as well as lamellar crystals can be simultaneously monitored by SAXS.<sup>20,24</sup> The results show that the critical strain  $\epsilon^*$  for inducing the appearance of shish is a constant, which does not vary with strain rate  $\dot{\epsilon}$  when the strain rate is sufficiently large to overcome the Rouse relaxation of the chains. This critical strain  $\epsilon^*$  leads the chain segments locked between two adjacent entanglement points to be extended, which demonstrates that the stretched network is responsible to shish formation instead of coil–stretch transition.

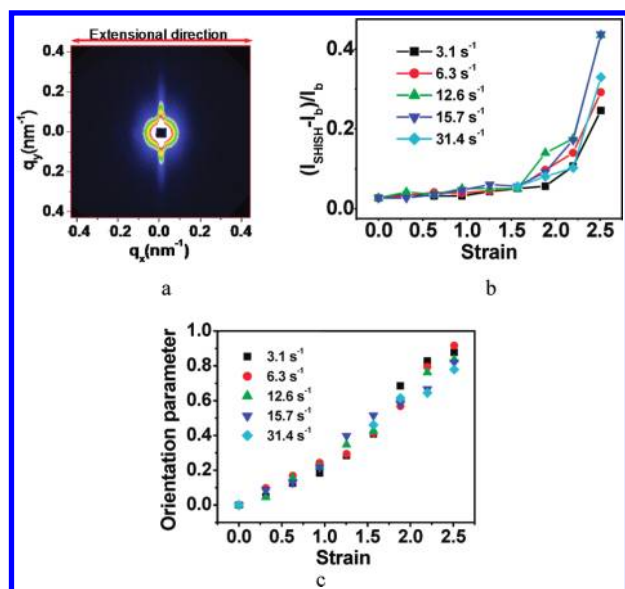
**Experimental Section.** A homemade miniature extensional rheometer is employed to impose stretching on high density polyethylene (HDPE) samples, which can be installed on the synchrotron radiation SAXS station for in situ measurements.

Figure 1 depicts a schematic picture of our homemade extensional rheometer, which is similar to SER designed by Sentmanat and allows us to obtaining the Hencky strain.<sup>25</sup> The ends of the sample are secured to the drums by means of clamps. The stretching object is the unsupported part of the sample with length of  $L_0$  which equals to the distance between the axes of the two drums. The stretching part  $L_0$  keep constant during test. With a constant angle velocity  $\omega$  of the drums the extensional strain rate is constant as  $\dot{\epsilon} = \Delta L/L_0 = 2\omega\pi d/L_0$ , where  $d$  is the diameter of the drums.<sup>25</sup> With this kind of extensional rheometer, the strain rate and the strain can be varied independently, which is crucial to justify the relation between the coil–stretch transition and shish formation as suggested by Keller.<sup>12</sup> The HDPE sample we used is supplied by Sinopec Qilu Co. Ltd. The sample has average molecular weights  $M_n$  and  $M_w$  of about 42 and 823 kg/mol, respectively. Rectangle shaped samples with length, width and thickness of 32, 20, and 0.8 mm, respectively, were used. After mounted on the drums of the rheometer by means of securing clamps, the samples were heated to 180 °C and held for 5 min to erase the possible thermal history, then the melt was cooled to 125 °C with a

\*Corresponding author. E-mail: lbli@ustc.edu.cn.



**Figure 1.** Schematic drawing of the extensional rheometer for in situ SR-SAXS measurements.



**Figure 2.** (a) Two-dimensional SR-SAXS pattern of HDPE after stretched with a strain and strain rate of 2.5 and  $15.7 \text{ s}^{-1}$ , respectively. The sharp meridional streak represents the formation of shish. (b) Plots of shish content vs strain at different strain rates. Shish does not appear until strain is larger than about 1.57. (c) Plots of orientation parameter of lamellar crystal vs strain at different extensional rates.

cooling rate of  $8 \text{ }^{\circ}\text{C}/\text{min}$ . Immediately after the temperature reached  $125 \text{ }^{\circ}\text{C}$ , extension with strain rates  $\dot{\epsilon}$  of 3.1, 6.3, 12.6, 15.7, and  $31.4 \text{ s}^{-1}$  were imposed on HDPE melt with different strains  $\epsilon$ , respectively. In situ SAXS measurements were conducted to monitor the formation of shish and lamellar crystals or kebab, which were carried out on the BL16B1 beamline in the Shanghai Synchrotron Radiation Facility (SSRF).

**Results and Discussion.** Figure 2a is a representative 2D SR-SAXS pattern of HDPE collected just after the cessation of extension with an extensional strain rate  $\dot{\epsilon}$  and strain  $\epsilon$  of  $15.7 \text{ s}^{-1}$  and 2.50 at  $125 \text{ }^{\circ}\text{C}$ , respectively. The extension is in the horizontal direction, as indicated with the arrow in the figure. The sharp meridional streaks represent the formation of shish. The kebab, represented by the equatorial scattering maximum, appeared after about 240 s. Note that in situ wide-angle X-ray scattering (WAXS) measurements show that shish is crystal with strong field while with a medium extension field it takes some time to crystallize. Further data processing shows that the length of shish is around 200 nm and the diameter is about 15 nm. The processing method has been described in detail elsewhere by Keum et al.<sup>26</sup> With increase of strain, the length of shish increases, while variation of strain rate does not show significant effect on shish length. With SR-SAXS patterns, we extracted the relative

content of initial shish just after the cession of extension as well as the orientation of the final kebab structure after the completion of crystallization. The relative content of the shish  $x_{\text{shish}}$  is defined with the following equation:

$$x_{\text{shish}} = (I_{\text{shish}} - I_b) / I_b \quad (1)$$

where  $I_{\text{shish}}$  is the scattering intensity of the streaks from the shish and  $I_b$  is the background scattering intensity from the melt. The orientation of the kebab is defined with Herman's orientational parameter  $f$ .

$$f = \frac{3\langle \cos^2 \phi \rangle - 1}{2}$$

$\phi$  is the angle between the flow direction and the lamellae orientation. The value of standard Herman's orientational parameter  $f$  is 0 when the lamellae direction distribution is isotropic, and the value is 1 when the lamellae are in perfectly alignment.

With different extensional strain rates, extensional strains smaller and larger than the yield strain  $\epsilon_y$  were imposed on supercooled HDPE melt at  $125 \text{ }^{\circ}\text{C}$ . The relative contents of shish  $x_{\text{shish}}$  are plotted vs extensional strain  $\epsilon$  in Figure 2b. With an extensional strain rate of  $3.1 \text{ s}^{-1}$ , shish appears only when the strain is larger than 1.88, while at larger strain rates and within experimental error, the extensional strain  $\epsilon$  required to induce shish formation is almost the same at about 1.57. Evidently, the critical extensional strain  $\epsilon^*$  to induce the formation of shish is a constant when the strain rate  $\dot{\epsilon}$  is sufficiently large.

Figure 2c presents the corresponding orientational parameters of lamellar crystals or kebab formed after being subjected with different strain rates and strains. The orientational parameters of kebab are nearly the same for a given strain  $\epsilon$  though the strain rate  $\dot{\epsilon}$  is varied. The orientational parameter increases with the increase of strain  $\epsilon$ , which exhibits a two-stage process. The transition of these two stages occurs at a strain  $\epsilon$  of about 1.5. With strains larger than about 1.5, the increase of the orientational parameter with strain  $\epsilon$  is accelerated with a larger slope than that at lower strains, which may indicate the enhancement of shish on the orientation of kebab.

Why is there a constant strain for the appearance of shish at different strain rates? Does this strain correspond to coil-stretch transition? Answering these questions may help us to resolve the molecular mechanism of shish formation, which we have to rely on rheological measurements.

Figure 3a plots the engineering stress vs time under extension with an extensional strain rate  $\dot{\epsilon}$  of  $6.2 \text{ s}^{-1}$  and different strains  $\epsilon$  at  $125 \text{ }^{\circ}\text{C}$ , respectively. As the stress relaxation is also recorded after the cession of extension, time  $t$  instead of strain  $\epsilon$  is used as the  $x$ -axis. We plot engineering stress rather than so-called true stress vs time based on the following two points. (i) Polymer melt acts like a solid when the extension rate is large enough to overcome relaxation of chain. Defining yield of polymer solid, engineering stress-strain curve rather than true stress-strain curve is employed. (ii) Stress of rubber network is determined by segment density  $n$  between two entanglement points rather than cross section area. If there is no disentanglement, it may not be proper to simply divide the cross section area. In the first stage of extension, the melt acts like elastic solid while responding to the external force and a large slope exhibits. Before yielding a reduction of slope is due to the consequence of Rouse relaxation. Yielding happens when the applied strain  $\epsilon$  is larger than the yield strain  $\epsilon_y$ , which indicates the occurrence of interchain

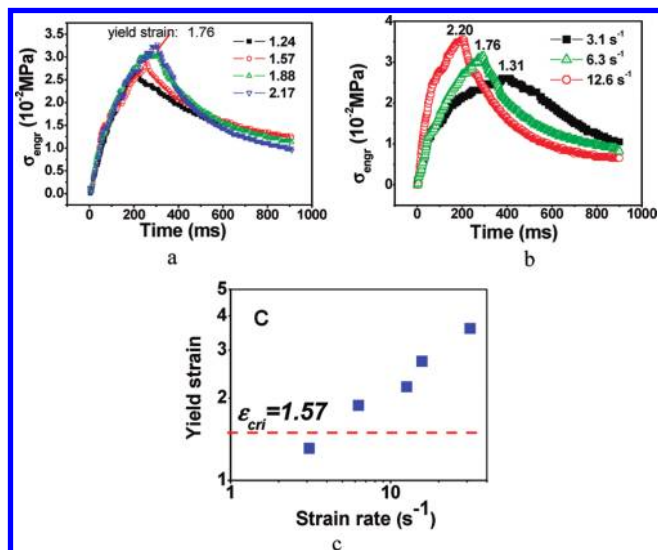


**Figure 3.** (a) Engineering stress–strain curves of supercooled HDPE melt with different strains at a strain rate of  $6.3 \text{ s}^{-1}$ . (b) Engineering stress–strain curves of supercooled HDPE melt with different strain rates. The numbers from 3.1 to  $12.6 \text{ s}^{-1}$  indicate the extensional rates, while the maximum of the stress indicates of the yield point. (c) Extensional yield strains vs strain rate. The red dash line indicates the critical strain  $\epsilon$  to induce shish formation.

slippage and disentanglement. With strains of 1.88 and 2.11, the stress maximum is identical at 1.76, which is the yield strain  $\epsilon_y$ , where chains start to move out from the original tubes to cause disentanglement. With a strain  $\epsilon$  lower than the yield strain, the relaxation of stress  $\sigma$  is much slower than that after yielding, which indicates the different relaxation kinetics of molecular chains in the entangled and disentangled states. We did not observe any poststretching yield or necking with a strain lower than the yield strain  $\epsilon_y$  for all strain rates we studied at this temperature.

The yield strain  $\epsilon_y$  varies with strain rates. Figure 3b depicts three representative extensional curves with different strain rates. Though the yielding occurs after longer extension time under smaller strain rate  $\dot{\epsilon}$ , the actual yield strain  $\epsilon_y$  increases with the increase of strain rate  $\dot{\epsilon}$ . Figure 3c plots the yield strain  $\epsilon_y$  or cohesive failure strain vs strain rate  $\dot{\epsilon}$ . With the increase of strain rate  $\dot{\epsilon}$ , the yield strain  $\epsilon_y$  increases. We indicate the critical strain  $\epsilon^*$  for the appearance of shish in Figure 3c with red dash line. Clearly the critical strain  $\epsilon^*$  of 1.57 is less than the yield strain  $\epsilon_y$  when the strain rate  $\dot{\epsilon}$  is large enough to overcome the Rouse relaxation of chain.

On the basis of the rheological data and experimental data of shish formation from SR-SAXS, we can draw a safe conclusion that the chains being stretched out from the original tube is not a necessary condition for shish formation. Note the transient polymer network may undergo poststretching yielding even with a strain less than the yield strain at  $180^\circ\text{C}$  where no crystallization takes place, but does not occur at  $125^\circ\text{C}$ . This clearly demonstrates that the formation of shish and crystallization prevents the supercooled HDPE melt from poststretching yielding, while the later does not play a role in shish formation as it does not occur at all. Evidently, chain-stretched out from the original tube or the coil–stretch transition is not responsible for shish formation in HDPE melt.

What happens at the molecular level when polymer melts under the critical strain  $\epsilon^*$  of about 1.57? The experimental results clearly point to the primary role of stretched network on shish formation. Evidently, the critical strain of 1.57 for shish formation in HDPE is certainly not large enough to

induce coil–stretch transition. Taking the average molecular weight of HDPE we used here, stretching the chain into a fully extended configuration requires a strain  $\epsilon$  of about 25. If full chain can not be stretched into extended configuration, can chain segments locked between two adjacent entanglement points be extended under the critical strain  $\epsilon^*$ ?

The entangled network responds to the external deformation like a solid, when the applied strain rate  $\dot{\epsilon}$  is larger than the inverse Rouse relaxation time  $\tau_R$ , namely Weissenberg number  $Wi = \epsilon \tau_R \geq 1$ .<sup>27</sup> The chain segments with the critical entanglement molecular weight  $M_e$  are locked by two adjacent entanglement points, which undergo nearly affine deformation at strain  $\epsilon$  lower than the yielding strain  $\epsilon_y$ . Thus, we made an approximate calculation on the deformation of chain segments with the simple affine model. Since the critical entanglement molecular weight  $M_e$  of HDPE is  $828 \text{ g/mol}$ ,<sup>28</sup> in the equilibrium Gaussian configuration the end-to-end distance of this polymer segment is  $\sqrt{\langle R^2 \rangle} = \sqrt{Nb^2} = 3.6 \text{ nm}$ . With all trans conformation, the length of the fully extended chain segment  $L_{ex}$  between two entanglement points is  $9.26 \text{ nm}$ . Thus, the ratio  $L_{ex}/\langle R^2 \rangle^{1/2}$  between the extended chain length  $L_{ex}$  and the end-to-end distance  $\langle R^2 \rangle^{1/2}$  in Gaussian configuration of the chain locked between two entanglement points is 2.57 for  $C_\infty = 7.4$  and 2.66 for  $C_\infty = 6.9$ , where  $C_\infty$  is the characteristic ratio.<sup>29</sup> The ratio  $L_{ex}/\langle R^2 \rangle^{1/2}$  matches remarkably well with the strain required to induce the formation of shish. Under the critical strain  $\epsilon^*$  for shish formation of about 1.57, the chain length between two entanglement points becomes 2.57 times of the initial end-to-end distance in Gaussian configuration, which exactly corresponds to the extended configuration. One may note the role of relaxation. Indeed during and after the stretching molecular chains always undergo relaxation and the chain configuration depends on the memory function and the deformation parameters like strain  $\epsilon$  and strain rate  $\dot{\epsilon}$ . Nevertheless, the memory function itself is a statistic analysis.<sup>30,31</sup> Thus, even taking into account the role of relaxation, some portion of chain segments locked between two adjacent entanglement points can still reach its nearly extended configuration with the critical strain  $\epsilon^*$  for shish formation. Within certain range either increasing strain  $\epsilon$  or strain rate  $\dot{\epsilon}$  increases the content of shish (Figure 2b), which is in line with the statistic rule. Moreover the formation of shish introduces a coupling among chain segments, which prevents the extended configuration from relaxing. This indeed is evidenced by that no necking occurs at temperature allowing shish formation while necking takes place well above the melting temperature with the same strain. The existence of the critical strain  $\epsilon^*$  unveils a molecular picture that extension of chain segment locked between two entanglement points is one necessary condition for shish formation in polymer melt. In another word, stretched network rather than the coil–stretch transition is the basis for shish formation in polymer melt. The idea of stretched network is in line with the early idea of Pennings,<sup>17</sup> which in fact brings the success of high performance ultrahigh molecular weight PE fiber. Shish formation in stretched rubber network is another strong evidence to support this idea which was reported long time ago.<sup>32</sup>

Though the stretched network is essential for the formation of shish, it may not be the only contributor. Indeed Kimata et al. show that shish contains not only long chains but also short chains.<sup>19</sup> Our early work based on end-linked PEO network also leads to the same conclusion for system without disentanglement.<sup>33</sup> The formation of shish or oriented nuclei is a synergistic effect of stretched network reducing nucleation barrier and short chain with fast



diffusion. This approach does not require the stretched segments to get together and pack into shish.

Stretched network as the basis of shish formation in polymer melt is manifested through the experimental results with the mixture of long and short chains.<sup>16,20–22</sup> Adding long chains into short chain matrix has been found to promote the formation of shish and accelerate the crystallization process. However it is well recognized that the amount of the long chains has to be larger than the overlapping concentration  $c^*$ , which clearly implies the importance of network in flow-induced crystallization of polymer melt. To ensure such an elastic deformation, the strain rate  $\dot{\epsilon}$  must be larger than the inverse of the Rouse relaxation time of long chains ( $W_i = \epsilon \dot{\epsilon} \tau_R \geq 1$ ), which must have a concentration larger than  $c^*$  for constructing the network. To check whether our HDPE with wide molecular distribution meet this requirement or not, we made a simple calculation as following. The Rouse time  $\tau_R = \tau_e Z^2$ , where  $\tau_e$  is the equilibration time ( $7 \times 10^{-9}$  s at 190 °C) and  $Z$  is the monomer number.<sup>23,24</sup> For the Rouse time equal to the reciprocal of the strain rate of  $3.1 \text{ s}^{-1}$ , the corresponding molecular weight is 4800K, which has a content of 4% in our HDPE samples according to GPC data. With this molecular weight, the overlapping concentration  $c^*$  is only 0.028%. This is far below the actual concentration of long chains, indicating that the concentration of chains with high enough molecular weight is far sufficient to form the network undergoing elastic deformation at such strain rates.

Finally, we come to the relation between the orientation of lamellar crystal and the formation of shish. At low strains, oriented lamellar crystals form without shish formation. Though the chain segments locked between two entanglement points are not fully extended, the weakly stretched network is sufficient to induce the formation of oriented lamellae. This structure may be the so-called row-structure defined by Keller and is consistent with the report of Zhang et al.<sup>18</sup> The orientational parameter of lamellae increases with the increase of strain  $\epsilon$ , but has no definite relation with the extensional strain rate  $\dot{\epsilon}$ . The specific work of shear on orientation of polymer crystal reported by Mykhaylyk and the specific strain for crystallization by Samon et al.<sup>34,35</sup> seems in line with current results. At low strains there is no shish formation to direct the growth of lamellae, thus the orientation parameter increases relatively slow with strain  $\epsilon$ . Once the shish forms, the kebab grows with the shish as the nuclei, which leads to an acceleration of the increase of lamellar orientation with strain  $\epsilon$ .

**Conclusion.** In conclusion, we combine the rheological method and the synchrotron radiation SAXS measurement to clarify the role of the coil–stretch transition and stretched network model on the formation of the shish. With a strain rate  $\dot{\epsilon}$  large enough to overcome the Rouse relaxation of chain, a critical strain  $\epsilon^*$  to induce shish formation is found to be a constant at different strain rates, which ensure fully extension of the chain segments locked between two adjacent entanglement points. Experimental evidence indicate that coil–stretch transition is not the necessary condition for shish formation in polymer melt. Instead, the stretched network is responsible for shish formation in polymer melt.

**Acknowledgment.** The authors would like to thank Prof. Shiqing Wang, Mr. Yangyang Wang (Akron) and

Prof. Gert Strobl (Freiburg) for fruitful discussion, Prof. Jie Wang, Dr. Yi Liu, and Dr. Yuzhu Wang for assistance on the SAXS experiments. This work is supported by the NNSFC (50973103, 20774091), the Fund for One Hundred Talented Scientists of CAS, the “NCET” Program of MOE, the 973 Program of MOST and the experimental fund of NSRL and SSRF.

## References and Notes

- (1) Peterlin, A. *Colloid Polym. Sci.* **1987**, *265*, 357–382.
- (2) Miller, R. L. *Flow-Induced Crystallization in Polymer Systems*; Gordon and Breach Science Publishers, Inc.: New York 1977.
- (3) Li, L. B.; De Jeu, W. H. *Adv. Polym. Sci.* **2005**, *181*, 75–120.
- (4) Hill, M. J.; Keller, A. J. *Macromol. Sci. B* **1969**, *3*, 153–169.
- (5) Mitsuhashi, S. *Bull. Text. Res. Inst.* **1963**, *66*, 1.
- (6) Pennings, A. J.; Kiel, A. M. *Kolloid Z. Z. Polym.* **1965**, *205*, 160–162.
- (7) Binsbergen, F. L. *Nature* **1966**, *211*, 516–517.
- (8) Kalb, B.; Pennings, A. J. *J. Mater. Sci.* **1980**, *15*, 2584–2590.
- (9) Ward, I. M. *Structure and properties of oriented polymers*; New York: Wiley; 1975.
- (10) Walczak, Z. K. *Processes of Fiber Formation*; Elsevier: Amsterdam, 2002.
- (11) de Gennes, P. G. *J. Chem. Phys.* **1974**, *60*, 5030–5042.
- (12) Keller, A. Kolnaar, H. W. H. *Flow Induced Orientation and Structure Formation*; VCH: New York, 1997; Vol. 18.
- (13) Zhu, P. W.; Edward, G. *Macromolecules* **2004**, *37*, 2658–2660.
- (14) Dukovski, I.; Muthukumar, M. *J. Chem. Phys.* **2003**, *118*, 6648–6655.
- (15) Wang, M.; Hu, W.; Ma, Y.; Ma, Y.-Q. *Macromolecules* **2005**, *38*, 2806–2812.
- (16) Kanaya, T.; Matsuba, G.; Ogino, Y.; Nishida; Shimizu, K. H. M.; Shinohara, T.; Oku, T.; Suzuki, J.; Otomo, T. *Macromolecules* **2007**, *40*, 3650–3654.
- (17) Smook, J.; Pennings, A. J. *J. Mater. Sci.* **1984**, *19*, 31–43.
- (18) Zhang, C. G.; Hu, H. Q.; Wang, X. H.; Yao, Y. H.; Dong, X.; Wang, D. J.; Wang, Z. G.; Han, C. C. *Polymer* **2007**, *48*, 1105–1115.
- (19) Kimata, S.; Sakurai, T.; Nozue, Y.; Kasahara, T.; Yamaguchi, N.; Karino, T.; Shibayama, M.; Kornfield, J. A. *Science* **2007**, *316*, 1014–1017.
- (20) Hsiao, B. S.; Yang, L.; Somani, R. H.; Avila-Orta, C. A.; Zhu, L. *Phys. Rev. Lett.* **2005**, *94*, 117802.
- (21) Zuo, F.; Keum, J. K.; Yang, L.; Somani, R. H.; Hsiao, B. S. *Macromolecules* **2006**, *39*, 2209–2218.
- (22) Seki, M.; Thurman, D. W.; Oberhauser, J. P.; Kornfield, J. A. *Macromolecules* **2002**, *35*, 2583–2594.
- (23) Wang, Y.; Wang, S. Q.; Boukany, P.; Wang, X. *Phys. Rev. Lett.* **2007**, *99*, 237801.
- (24) Balzano, L.; Kukalyekar, N.; Rastogi, S.; Peters, G. W. M.; Chadwick, J. C. *Phys. Rev. Lett.* **2008**, *100*, 048302.
- (25) Sentmanat, M.; Wang, B. N.; McKinley, G. H. *J. Rheol. (N.Y.)* **2005**, *49*, 585–606.
- (26) Keum, J. K.; Zuo, F.; Hsiao, B. S. *Macromolecules* **2008**, *41*, 4766–4776.
- (27) van Meerveld, J.; Peters, G. W. M.; Hütter, M. *Rheol. Acta* **2004**, *44*, 119–134.
- (28) Fetters, L. J.; Lohse, D. J.; Richter, D.; Witten, T. A.; Zirkelt, A. *Macromolecules* **1994**, *27*, 4639–4647.
- (29) Fang, J. N.; Kröger, M.; Öttinger, H. C. *J. Rheol.* **2000**, *44*, 1293–1317.
- (30) Doi, M. Edwards, S. F. *The Theory of Polymer Dynamics*; Clarendon Press: Oxford, U.K., 1986.
- (31) Azzurri, F.; Alfonso, G. C. *Macromolecules* **2005**, *38*, 1723–1728.
- (32) Andrews, E. H.; Reeve, B. J. *Mater. Sci.* **1971**, *6*, 547–557.
- (33) Zhao, B. J.; Li, X. Y.; Huang, Y. J.; Cong, Y. H.; Ma, Z.; Shao, C. C.; An, H. N.; Yan, T. Z.; Li, L. B. *Macromolecules* **2009**, *42*, 1428–1432.
- (34) Samon, J. M.; Schultz, J. M.; Hsiao, B. S. *Polymer* **2002**, *43*, 1873–1875.
- (35) Mykhaylyk, O. O.; Chambon, P.; Graham, R. S.; Fairclough, J. P. A.; Olmsted, P. D.; Ryan, A. J. *Macromolecules* **2008**, *41*, 1901–1904.